NASA-CR-165407
IITRI-M06001-89

THERMAL FATIGUE AND OXIDATION DATA OF TAZ-8A AND M22 ALLOYS AND VARIATIONS

by

K. E. Hofer and V. E. Humphreys
Materials Technology Division

IIT RESEARCH INSTITUTE
10 West 35th Street
Chicago, Illinois 60616

Prepared for

NATIONAL AERONAUTICS AND SPACE ADMINISTRATION

September 1981

CONTRACT NAS3-17787

NASA-Lewis Research Center
Cleveland, Ohio

Peter T. Bizon, Project Manager

1 Report No	2 Government Accession No	3 Recipient's Catalog No
NASA-CR-165407		

4 Title and Subtitle	5 Report Date
THERMAL FATIGUE AND OXIDATION DATA OF TAZ-8A AND M22 ALLOYS AND VARIATIONS	September 1981
	6 Performing Organization Code
7 Author(s)	8 Performing Organization Report No
K. E. Hofer and V. E. Humphreys	IITRI-M06001-89
	10 Work Unit No
9 Performing Organization Name and Address	
IIT Research Institute 10 West 35th Street Chicago, Illinois 60616	11 Contract or Grant No NAS3-17787
	13 Type of Report and Period Covered Contractor Report
12 Sponsoring Agency Name and Address National Aeronautics and Space Administration Washington, D.C. 20546	14 Sponsoring Agency Code

15 Supplementary Notes

Project Manager, Peter T. Bizon, Structures and Mechanical Technologies Division, NASA-Lewis Research Center, Cleveland, Ohio 44135

16 Abstract

Thermal fatigue and oxidation data were obtained on 36 specimens, representing 18 distinct variations (including the base systems) of TAZ-8A and M22 alloys. Double-edge wedge specimens for these systems were cycled between fluidized beds maintained at 1088°C and 316°C with a 180 s immersion in each bed. The systems included alloys TAZ-8A, M22, and 16 variations of these alloys. Each alloy variation consisted of a unique composition with an alteration in the percentage of carbon (C1 and C2), molybdenum (M1 and M2), tungsten (W1 and W2), columbium (CB1, CB2, and CB3), tantalum (T1, T2, and T3), or boron (B1, B2, and B3) present. All of the alloys showed little weight change due to oxidation compared with other alloys previously tested in fluidized beds. Only both C1 alloy variation specimens survived 3500 cycles without cracking in the small radius, although substantial cracks were present, emanating from the end notches which were used for holding the specimens.

17 Key Words (Suggested by Author(s))		18 Distribution Statement
TAZ-8A	Thermal Resistance	Unclassified - Unlimited
M22	Thermal Fatigue	
Oxidation	Nickel Alloys	
Fluidized Bed	Superalloys	
Heat Resistance Alloys	Mechanical Properties	

19 Security Classif (of this report)	20 Security Classif (of this page)	21 No of Pages	22 Price*
Unclassified	Unclassified	44	$3.00

* For sale by the National Technical Information Service Springfield Virginia 22161

FOREWORD

This report describes the results of thermal fatigue and oxidation testing of Series 5 test specimens on NASA Contract NAS3-17787. The report covers part of the work conducted on this contract during the period 1 February to 30 April 1980. Other IITRI work on fluidized bed thermal fatigue testing has been reported in NASA CR-72738, CR-121211, CR-134775, CR-135272, CR-135299, CR-159798, and CR-159842.

Peter T. Bizon was the NASA-Lewis Research Center Project Manager. IITRI personnel assigned to this program included K. E. Hofer (Project Manager, Materials Technology Division), V. E. Humphreys (Project Engineer), M. Yerman (Contract Specialist), D. Brown, and V. Johnson.

The IITRI internal designation for this report is IITRI-M06001-89. Thermal fatigue and oxidation data contained in this report are recorded in Logbook Nos. C24970 and C25141.

TABLE OF CONTENTS

LIST OF TABLES

LIST OF FIGURES

SUMMARY

Thermal fatigue and oxidation testing described in this report are part of a general study of thermal fatigue being conducted by the NASA-Lewis Research Center. Earlier work in the study has been reported in NAS CR-72738, CR-121211, CR-121212, CR-134775, CR-135272, CR-135299, CR-159798, and CR-159842. All testing on this contract has been conducted employing flüidized bed heating and cooling. The testing reported herein was over the temperature range 1088°C/316°C with a 180 s immersion in each fluidized bed employing double-edge wedge specimens.

Thermal fatigue and oxidation data were obtained on 36 specimens representing 18 alloys and compositional variations, including the two basic systems of TAZ-8A and M22 alloys. All of the systems were examined in the bare condition.

Both of the C1 alloy variation specimens survived 3500 thermal cycles without cracking on the small radius of the double-edge wedge specimen, but a substantial longitudinal crack was present, emanating from the end notches. Compared to other alloys previously examined, all of these alloys exhibited little weight change.

1. INTRODUCTION

This report, NAS CR-165407, on Contract MAS3-17787, summarizes thermal fatigue and oxidation data for 36 double-edge wedge specimens of TAZ-8A and M22 alloys, and 16 variations. The specimens of double-edge wedge cross-section were cycled in a fluidized bed facility over the temperature range of 1088°/316°C (1990°/600°F) up to a maximum of 3500 cycles. The heating and cooling times were always 180 s each. Weight changes, as well as cycles-to-crack initiation and crack propagation, were obtained during this phase of the program.

Thermal fatigue data obtained previously have been reported on this contract.[1-3] Additional thermal fatigue data obtained in the IITRI fluidized bed have been reported on Contracts NAS3-14311,[4-6] NAS3-18942,[7] and NAS3-19696.[8] This effort comprises part of the general study of thermal fatigue being conducted by the NASA-Lewis Research Center. Further details of the study have been reported by Spera, et. al.,[9,10] Bizon, et. al.,[11-13] and Howes.[14]

Any material exposed to repeated rapid thermal transients is subjected to tensile failure by thermal fatigue, also sometimes defined as thermal shock. The thermal fatigue degradation mechanism involves accumulation of damage during multiple thermal cycles. Thermal shock, on the other hand, generally involves failure in relatively few cycles. The difference generally lies in the tensile ductility of the material within the temperature range of the imposed thermal cycle. Ductile materials tend to fail by thermal fatigue, whereas brittle materials fracture by thermal shock.

Material properties, other than ductility, important in thermal fatigue are hot tensile strength, elastic modulus, thermal conductivity, and thermal expansion. Oxidation resistance apparently also plays a role in thermal fatigue. The interrelationship of material properties, imposed thermal cycle, and component geometry defines the ability of a structure to resist thermal fatigue. However, the synergistic effects of these variables are quite complex, and prediction of thermal fatigue behavior from basic properties is difficult. A major objective of the current NASA-Lewis Research Center's fatigue program is to develop and verify a usable model for thermal fatigue by comparing experimental data with computer-derived predictions of thermal fatigue life.

Thermal fatigue data in this report were generated using a multiple retort fluidized bed test facility consisting of one heating bed and two cooling beds. Glenny and co-workers reported the first use of fluidized beds to study thermal fatigue.[15]

Fluidized bed heating and cooling provide very rapid heat transfer for both portions of the thermal cycle. An additional advantage of fluidized bed testing is that it provides a ready means of simultaneously exposing a large number of samples under identical test conditions. In this program, up to 36 test specimens were exposed simultaneously.

The objective of the thermal fatigue test program was threefold:

1) Determine the number of imposed thermal cycles to initiation of the first transverse crack.

2) Obtain data on the rate of propagation of the three largest cracks for each specimen.

3) Generate qualitative oxidation data for the various materials.

Cycling of test specimens was generally continued until the three largest cracks reached a length of about 10 mm (0.4 in.). This corresponds to the approximate width of the tapered section of the test specimen. In some cases, exposure of specimens was continued in order to obtain oxidation data for specific alloys.

2. EXPERIMENTAL PROCEDURE

2.1 Materials

Thermal fatigue testing in this program was performed on 36 specimens of bare TAZ-8A and M22 alloys, and 15 compositional variations. The intended compositional variations and the actual compositions are shown in Table 1. All test specimens and compositional data were supplied by NASA-Lewis Research Center.

Tensile properties at 760°C (1400°F) and stress-rupture properties at 982°C (1800°F) of the test alloys are summarized in Table 2 and 3, respectively. These data were generated at the NASA-Lewis Research Center using specimens fabricated from the same heats of the alloys as that used to fabricate the thermal fatigue specimens.

2.2 Test Facility and Procedure

The fluidized bed thermal fatigue test facility is shown schematically in Figure 1. This equipment includes one hot bed mounted between two cold, or intermediate, temperature beds. Both intermediate temperature beds were employed in this program. For testing near ambient temperatures the lower bed temperature is maintained by a water-cooled heat exchanger. However, for testing at the 316°C (600°F) intermediate bed temperature in this program, the heat exchanger was removed, and the desired intermediate bed temperature was maintained by heating elements. Heat transfer media in both hot and cold beds was 28-48 mesh tabular alumina.

During testing in this program, up to 36 test specimens were cycled simultaneously using two coupled holding fixtures. At any time during testing, one holding fixture was in the hot bed and the other in either of the two intermediate beds. The transfer carriage, operated by air cylinders, can be programmed for any combination of heating and cooling times. Transfer time between beds was less than 5 s, and heating and cooling times were 180 s each for the test program reported herein.

Thermal fatigue data in this program was obtained using nominal 102 mm long double-edge wedge simulated blade shape mounted in a holding fixture, both as shown in Figure 2. Test specimens were supported using 6.3 mm wide notches machined 7 mm deep in the ends of the specimen. The notches provided ease of fixture fabrication, as well as simple removal of specimens for examination. In addition, the potential for superimposition of mechanical stresses due to the fixture was minimized.

The holding fixture, shown in Figure 2, capable of retaining 18 test specimens, was fabricated from austenitic stainless steel. End plates were 12.7 mm thick 310 stainless steel with a radius 0.25 mm less than the specimen notches. The side supports were fabricated from 304 stainless steel channel. During testing, the test fixture also generated thermal fatigue cracks and required frequent replacement.

Thermal fatigue testing was conducted by cycling two holders containing a total of 36 test specimens up to a maximum of 3500 cycles. In addition, dummy samples were mounted at each end of the holder to eliminate end effects. Of the original 36 test specimens, only 8 completed the full 3500 cycles. The remaining 28 samples were removed earlier because of excessing cracking. Three specimens were removed after 1500 cycles, 17 after 2500 cycles, and 8 after 3000 cycles.

During testing at 1088°/316°C (1990°/600°F), specimens were removed and inspected after selected intervals for gravimetric analysis and crack length measurements. These nominal intervals were 25, 50, 100, 200, 300, 500, 700, and 1000 cycles, with subsequent examination after every 500 cycles for exposure greater than 1000 cycles. Length of the three longest cracks was determined visually using a microscope at 30X. The number of cycles to crack initiation was taken as the average of the number of cycles at the last inspection without cracks and the number of cycles at the first inspection with a crack. However, specimens were generally retained in the test program after crack initiation to obtain additional oxidation and crack propagation data.

Table 4 summarizes the dimensions and identification of the 36 test specimens evaluated in this program. Both the initial (as-received) and final dimensions are shown. Data on total thermal cycles imposed on each specimen are included for reference.

3. RESULTS

3.1 Oxidation Behavior

Weight change data for the 36 test specimens are contained in Table 5. Figures 3 to 8 are plots of the oxidation data for these same specimens.

Oxidation data in Table 5 and Figures 3 to 8 are expressed in percent of the original weight, since oxidation was not uniform over the test specimen. In general, the majority of the oxidation occurred on the wedge areas of the specimen. This is because these areas were exposed to the maximum temperature of the thermal cycle for longer periods than the thicker center section of the specimen. Thermocouple calibration tests reported in NASA CR-121211 indicated that for double-edge wedge specimens cycled in fluidized beds, the center section of the specimen is nominally 17° to 30°C (31° to 54°F) less than the maximum temperature of the wedge section at the end of a 180 s heating cycle.

Thermocouple calibration data also indicate that the wedge sections of the specimen were within 25°C of the 1088°C maximum temperature for the average time of about 75 s, at the end of the 180 s heating cycle. Qualitatively, therefore, the cumulative exposure was equivalent to about 20 hr at 1088° ± 25°C (1990° ± 45°F) for each 1000 cycles of testing. This corresponds to 70 hr for 3500 cycles exposure. Rapid thermal cycling, however, accelerates oxidation significantly in comparison to isothermal exposure.

Overall, the oxidation of all of the TAZ-8A and M22 alloy variations was less than most alloys previously studied.[1-5] None of the weight losses or gains exceeded 0.1% of the original weights and, indeed, most weight changes lay within the bounds of the basic TAZ-8A and M22 alloys.

In short, the oxidation resistance of alloys varying slightly from the base TAZ-8A and M22 alloys is at least as good and generally better than the base alloys. Since all weight changes were small compared to that determined in previous thermal fatigue tests, the comparisons above should be made only with the overall thermal cycling data taken into consideration (i.e., thermal crack growth).

3.2 Thermal Fatigue Resistance

Accumulated thermal cycles to first crack initiation for the TAZ-8A and M22 alloys and variations tested are summarized in Table 6. In this table, the cycles to first crack initiation on both the 0.64 mm small radius and on the 1.02 mm large radius are included for comparison. Generally, cracking of the large radius is of lesser importance, particularly if preceded by cracking of the small radius. The emergence of thermal cracks on the small radius influences the stress distribution in the specimen. This can increase the cycle time to initiation of cracks on the large radius.

"Cycles to first crack" in Table 6 is based on the average between the last inspection period without a crack and the inspection period at which a crack was first visible. For example, if no cracks were observed at 100 cycles but became visible at 200 cycles, origination of the first crack is considered to be 150 cycles. Accordingly, thermal fatigue data in Table 6 have an inherent potential error varying from ±12 cycles to ±150 cycles for exposure less than 1000 cycles. The error is ±250 cycles for exposures above 1000 cycles, based on the inspection periods described previously.

Table 7 contains optically measured crack lengths for the three longest cracks on each TAZ-8A and M22 alloy and variation specimen as a function of accumulated cycles. Crack lengths shown are measured on both wedge surfaces and are averaged to obtain the average crack length. Each of the cracks is located in relation to the bottom (numbered end) of the test specimen. Also identified in this table is the total number of cracks observed on both the small (0.64 mm) and large (1.02 mm) radii.

Figures 9 and 10 show the as-received appearance of typical experimental TAZ-8A and M22 alloys and variations. Figure 11 shows the appearance of typical specimens after thermal cycling. In all photographs, the small radius is at the right.

Fatigue data in Tables 6 and 7 indicate that the lowest fatigue resistance was exhibited by the alloy M22 itself and both the T1 and B2 alloy variations where cracking occurred in the small radius after 850 cycles for the alloys. In addition, the M22 base alloy also exhibited cracking in the large radius after 850 cycles. The highest thermal fatigue crack resistance was shown by the C1 alloy variation which did not crack in the wedge portions after 3500 cycles. However, as shown in Figure 11, large cracks emanated from the notches of these specimens. Longitudinal notch cracks in Specimens C1-1 and C1-4 were first notices during the 2000-2500 cycle examination. Notch crack length at this time were approximately 25 mm. After completion of the test series at 3500 cycles, the maximum notch crack length had grown to 42.8 mm. Longitudinal cracks developed in the specimen support notches would reduce the accumulated thermal stresses developed in thermal cycling of specimens C1-1 and C1-4. This would, in effect, delay the development of transverse cracks in the small and large radii of the specimens. In addition, Specimen 2 of the CB3 alloy variation did not crack until after 3250 cycles. Its corollary sample, Specimen 1, cracked at 2750 cycles. Similar behavior was noted for alloy variation M2, with cracking at 3250 and 2250 cycles for the two specimens tested.

Ranking the alloys in terms of small radius crack initiation results in the following order of increasing fatigue resistance: M22, B2, T1, B3, W2, W1, T3, M1, T2, CB2, CB1, B1, TAZ-8A, W3, CB3, and C1.

4. SUMMARY OF RESULTS

The thermal fatigue crack resistance and oxidation data on the 36 TAZ-8A and M22 alloys and variations tested in fluidized beds maintained at 1088°/316°C indicate the following conclusions:

1) The TAZ-8A and M22 alloys and the compositional variation alloys all possessed an excellent oxidation resistance. The variational alloys showed weight changes between the two extreme positions exhibited by TAZ-8A which lost weight and M22 which gained weight.

2) The highest resistance to thermal fatigue cracking appeared to be exhibited by C1 specimens which, at least up to the 3500 cycle limit of testing, did not crack in the wedge sections of the double-edge wedge specimens. However, large cracks originated at the holding notches for these specimens.

3) The least resistance to thermal fatigue cracking appeared to be exhibited by M22 alloy and T1 and B2 variations, which cracked prior to attaining 1000 cycles.

REFERENCES

1. M. A. H. Howes, "Thermal Fatigue and Oxidation Data on TAZ-8A, MAR-M 200, and Udimet 700 Superalloys," NASA CR-134775, 1975.

2. V. L. Hill and V. E. Humphreys, "Thermal Fatigue and Oxidation Data of Superalloys Including Directionally Solidified Eutectics," NASA CR-135272, June 1977.

3. K. E. Hofer, V. L. Hill and V. E. Humphreys, "Thermal Fatigue and Oxidation Data of Oxide Dispersion-Strengthened Alloys," NASA CR-159842, March 1980.

4. M. A. H. Howes, "Thermal Fatigue Data on 15 Nickel- and Cobalt-Base Alloys," NASA CR-72738, 1970.

5. M. A. H. Howes, "Additional Thermal Fatigue Data on Nickel- and Cobalt-Base Superalloys," Part 1, NASA CR-121211, 1973.

6. M. A. H. Howes, "Additional Thermal Fatigue Data on Nickel- and Cobalt-Base Superalloys," Part 2, NASA CR-121212, 1973.

7. V. L. Hill and V. E. Humphreys, "Thermal Fatigue and Oxidation Data for Alloy/Braze Combinations," NASA CR-135299, 1977.

8. V. L. Hill and V. E. Humphreys, "Thermal Fatigue and Oxidation Data for Directionally Solidified MAR-M 246 Turbine Blades," NASA CR-159798, 1980.

9. D. A. Spera and S. J. Grisaffe, "Life Prediction of Turbine Components: On-Going Studies at the NASA-Lewis Research Center," NASA TM X-2664, 1973.

10. D. A. Spera, M. A. H. Howes and P. T. Bizon, "Thermal Fatigue Resistance of 15 High-Temperature Alloys Determined by the Fluidized-Bed Technique," NASA TM X-52975, March 1971.

11. P. T. Bizon and R. E. Oldrieve, "Thermal Fatigue Resistance of NASA WAZ-20 Alloy with Three Commercial Coatings," NASA TM X-3168, 1975.

12. P. T. Bizon and D. A. Spera, "Thermal-Stress Fatigue Behavior of Twenty-Six Superalloys," ASTM Special Technical Publication 612, pp. 106-122, 1976.

13. P. T. Bizon and D. A. Spera, "Comparative Thermal Fatigue Resistance of Twenty-Six Nickel- and Cobalt-Base Alloys," NASA TN D-8071, 1975.

14. M. A. H. Howes, "Evaluation of Thermal Fatigue Resistance of Metals Using the Fluidized-Bed Technique," ASTM Special Technical Publication 520, pp. 242-254, 1973.

15. E. Glenny, J. E. Northwood, S. W. K. Shaw and T. A. Taylor, "A Technique for Thermal-Shock and Thermal-Fatigue Testing Based on the Use of Fluidized Solids," J. Inst. Metals, Vol. 87, pp. 294-302, 1958-1959.

TABLE 1. INTENDED AND ACTUAL COMPOSITIONS OF TAZ-8A AND M22 ALLOYS AND VARIATIONS

Alloy	Composition Type	Heat No.	Composition, wt. %									
			C	Mo	W	Cb	Ta	B	Cr	Al	Zr	Ni
TAZ-8A	intended	--	0.13	4.0	4.0	2.0	8.0	0.004	6.0	6.0	0.6	bal
	actual	X356	0.14	3.7	4.5	1.6	8.2	<0.001	6.1	6.4	0.57	bal
M22	intended	--	0.13	2.0	11.0	0	3.0	0	5.7	6.3	0.6	bal
	actual	X340	0.10	1.84	11.2	0	3.7	0.005	5.9	6.3	0.53	bal
C1	intended	--	0	4.0	4.0	2.0	8.0	0.004	6.0	6.0	0.6	bal
	actual	X344	0	3.4	4.7	1.9	7.4	<0.001	6.2	6.5	0.57	bal
C2	intended	--	0.065	4.0	4.0	2.0	8.0	0.004	6.0	6.0	0.6	bal
	actual	X342	0.13	3.6	4.6	1.8	8.0	<0.001	6.3	6.8	0.56	bal
M1	intended	--	0.13	0	4.0	2.0	8.0	0.004	6.0	6.0	0.6	bal
	actual	X345	0.09	0	4.1	1.9	7.6	<0.001	6.5	6.8	0.52	bal
M2	intended	--	0.13	2.0	4.0	2.0	8.0	0.004	6.0	6.0	0.6	bal
	actual	X348	0.16	1.9	4.4	1.6	7.1	<0.001	6.3	6.6	0.59	bal
W1	intended	--	0.13	4.0	0	2.0	8.0	0.004	6.0	6.0	0.6	bal
	actual	X346	0.14	3.8	0	1.8	7.4	<0.001	6.5	6.2	0.59	bal
W2	intended	--	0.13	4.0	7.5	2.0	8.0	0.004	6.0	6.0	0.6	bal
	actual	X343	0.13	3.4	8.4	1.7	8.2	<0.001	6.0	6.3	0.59	bal
W3	intended	--	0.13	4.0	11.0	2.0	8.0	0.004	6.0	6.0	0.6	bal
	actual	X341	0.09	3.5	11.9	1.7	8.1	0.006	5.5	6.0	0.55	bal
CB1	intended	--	0.13	4.0	4.0	0	8.0	0.004	6.0	6.0	0.6	bal
	actual	X347	0.18	3.6	4.3	0	7.4	<0.001	6.6	6.5	0.57	bal

TABLE 1. (Cont.)

Alloy	Composition Type	Heat No.	Composition, wt. %									
			C	Mo	W	Cb	Ta	B	Cr	Al	Zr	NI
CB2	intended	--	0.13	4.0	4.0	1.0	8.0	0.004	6.0	6.0	0.6	bal
	actual	X351	0.15	3.7	4.6	0.7	7.1	<0.001	6.3	6.5	0.56	bal
CB3	intended	--	0.13	4.0	4.0	3.0	8.0	0.004	6.0	6.0	0.6	bal
	actual	X352	0.10	3.3	4.9	3.3	7.2	<0.001	5.3	6.4	0.6	bal
T1	intended	--	0.13	4.0	4.0	2.0	0	0.004	6.0	6.0	0.6	bal
	actual	X350	0.25	4.1	4.4	2.1	0	<0.001	7.0	6.2	0.64	bal
T2	intended	--	0.13	4.0	4.0	2.0	3.0	0.004	6.0	6.0	0.6	bal
	actual	X353	0.24	3.8	4.3	1.9	3.8	<0.001	6.6	6.1	0.62	bal
T3	intended	--	0.13	4.0	4.0	2.0	5.5	0.004	6.0	6.0	0.6	bal
	actual	X354	0.17	3.8	4.3	1.7	5.0	<0.001	6.3	6.3	0.57	bal
B1	intended	--	0.13	4.0	4.0	2.0	8.0	0	6.0	6.0	0.6	bal
	actual	X355	0.13	3.7	4.6	1.6	7.3	<0.001	6.0	6.4	0.53	bal
B2	intended	--	0.13	4.0	4.0	2.0	8.0	0.002	6.0	6.0	0.6	bal
	actual	X357	0.14	3.4	4.1	1.7	7.5	<0.001	6.1	5.5	0.59	bal
B3	intended	--	0.13	4.0	4.0	2.0	8.0	0.01	6.0	6.0	0.6	bal
	actual	X358	0.16	3.5	4.2	1.9	7.0	0.02	6.2	5.5	0.60	bal

TABLE 2. TENSILE PROPERTIES OF TAZ-8A AND M22 ALLOYS AND VARIATIONS AT 760°C (1400°F)

Alloy/Heat		Tensile Properties: Proportional Limit MN/m²	ksi	Tensile Properties: Ultimate Tensile Strength MN/m²	ksi	Reduction of Area, %	Ductility*
T8A	X356	838	121.6	1048	152.0	5.8	.0598
M22	X340	747	108.3	943	136.7	7.9	.0824
M1	X345	756	109.6	1002	145.4	8.0	.0835
M2	X348	843	122.3	1052	152.6	4.8	.0497
W1	X346	725	105.2	965	140.0	6.4	.0666
W2	X343	951	138.0	962	139.5	0.8	.0075
W3	X341	752	109.0	752	109.0	0.6	.0059
CB1	X347	743	107.7	955	138.5	5.1	.0526
CB2	X351	794	115.1	971	140.9	4.0	.0412
CB3	X352	919	133.3	1074	155.8	1.7	.0169
T1	X350	705	102.2	888	128.8	6.0	.0623
T2	X353	721	104.5	963	139.7	8.3	.0861
T3	X354	745	108.0	925	134.2	4.5	.0458
B1	X355	800	116.0	1014	147.0	3.9	.0394
B2	X357	783	113.5	1047	151.9	8.1	.0846
B3	X358	723	104.8	952	138.1	4.1	.0417

All results are average of duplicate tests.

Crosshead speed = 2.5 mm (0.1 in.)/min.

*Ductility = $\ln \left(\frac{100}{100 - \text{Reduction of Area in Percent}} \right)$.

TABLE 3. SUMMARY OF 982°C (1800°F) STRESS-RUPTURE PROPERTIES

Alloy/Heat		Stress-Rupture Properties: MN/m^2	ksi	Time to Rupture, hrs	Average Life, hrs	Reduction of Area, %	Ductility[a]
T8A	X356	124	18	98, 118	108	5.8	.0602
M22	X340	124	18	142, 80	111	1.3	.0128
M1	X345	124	18	298, 283	290	6.9	.0716
M2	X348	124	18	40, 30	35	4.0	.0409
W1	X346	124	18	108, 134	121	6.7	.0690
W2	X343	124	18	71, 88	80	5.9	.0609
W3	X341	124	18	53, 50	52	5.8	.0592
CB1	X347	124	18	127, 193	160	2.3	.0227
CB2	X351	124	18	171, 125	148	2.8	.0283
CB3	X352	124	18	91, 85	88	6.5	.0670
T1	X350	124	18	196, 173	185	16.1	.1760
T2	X353	124	18	304, 389	347	9.8	.1026
T3	X354	124	18	128, 159	144	4.9	.0502
B1	X355	124	18	128, 108	118	6.6	.0683
B2	X357	124	18	179, 170	175	2.4	.0236
B3	X358	124	18	185, 172	179	6.0	.0617

[a] $\text{Ductility} = \ln \dfrac{100}{100 - \text{Reduction of Area in Percent}}$

TABLE 4. DIMENSIONS AND IDENTIFICATION OF TEST SPECIMENS

Alloy	Specimen Identi- fication	Measured Radius, mm		Initial Dimension, mm			Total Test Cycles	Final Dimension, mm		
		Small	Large	Length	Width	Thickness		Length	Width	Thickness
TA8	2	.71	.94	102.6	31.32	6.29	3500	102.06	31.39	6.32
TA8	4	.71	.97	102.11	31.34	6.25	3500	102.08	31.39	6.28
TA8	5	.69	1.02	102.08	31.34	6.35	3500	102.06	31.42	6.36
M22	2	.66	1.04	102.03	31.34	6.30	1500	102.01	31.39	6.31
M22	3	.66	1.07	102.01	31.27	6.32	1500	102.01	31.29	6.34
M22	4	.66	1.02	102.08	31.29	6.34	1500	102.03	31.32	6.33
B1	2	.56/.61	1.04	101.93	31.29	6.34	3000	101.96	31.39	6.36
B1	5	.61/.71	1.09	101.98	31.34	6.32	3000	101.93	31.39	6.38
B2	2	.66	.99	102.06	31.32	6.35	2500	102.06	31.39	6.37
B2	3	.66	.97	102.06	31.32	6.32	2500	102.08	31.39	6.33
B3	3	.66	1.07	101.93	31.37	6.30	2500	101.90	31.42	6.34
B3	5	.61	1.07	101.90	31.32	6.33	3000	101.93	31.39	6.38
CB1	4	.64	1.07	102.06	31.37	6.28	2500	102.08	31.37	6.29
CB1	5	.66	.99	102.01	31.29	6.30	3000	102.03	31.37	6.32
CB2	4	.69	.91	101.95	31.34	6.30	2500	101.90	31.42	6.33
CB2	5	.69	.99	102.01	31.29	6.33	2500	102.01	31.32	6.37
CB3	1	.66	1.07	102.11	31.34	6.37	3000	102.08	31.39	6.40
CB3	2	.64	1.04	102.18	31.37	6.32	3500	102.11	31.37	6.35
W1	3	.69	1.07	102.06	31.37	6.33	3500	102.03	31.50	6.37
W1	4	.71	1.09	102.06	31.32	6.37	3000	102.03	31.39	6.39
W2	2	.66	.97	102.01	31.29	6.32	2500	101.98	31.32	6.36
W2	3	.66	1.07	101.88	31.32	6.30	2500	101.83	31.34	6.33

TABLE 4. (Cont.)

Alloy	Specimen Identi-fication	Measured Radius, mm Small	Large	Initial Dimension, mm Length	Width	Thickness	Total Test Cycles	Final Dimension, mm Length	Width	Thickness
W3	1	.69	1.09	101.98	31.29	6.46	3000	101.98	31.34	6.48
W3	5	.76	1.04	101.98	31.32	6.44	3000	101.98	31.37	6.46
T1	3	.69	1.09	101.88	31.22	6.31	2500	101.90	31.29	6.34
T1	5	.66	1.07	101.83	31.19	6.33	2500	101.83	31.24	6.34
T2	1	.66	1.07	102.06	31.29	6.29	2500	101.98	31.34	6.30
T2	3	.69	1.04	101.98	31.32	6.28	2500	101.96	31.37	6.30
T3	1	.69	1.07	101.83	31.29	6.33	2500	101.80	31.34	6.34
T3	3	.69	1.02	101.78	31.29	6.33	2500	101.78	31.32	6.36
M1	3	.61	.97	101.90	31.27	6.33	2500	101.80	31.29	6.35
M1	4	.69	.89	101.93	31.24	6.35	2500	101.88	31.27	6.38
M2	2	.71	.99	102.01	31.37	6.39	2500	101.96	31.37	6.36
M2	5	.71	1.04	101.96	31.32	6.36	3500	101.90	31.34	6.38
C1	1	.66	.86	101.90	31.37	6.34	3500	101.85	31.39	6.36
C1	4	.66	.91	101.98	31.34	6.33	3500	101.88	31.37	6.35

TABLE 5. WEIGHT CHANGE DATA FOR TAZ-8A AND M22 ALLOYS AND VARIATIONS

Material	Sample Identification	Starting Weight, g	Weight Change at Given Cycles, %												
			25	50	100	200	300	500	700	1000	1500	2000	2500	3000	3500
TA8	2	125.0157	.001	.002	.003	.005	.003	.008	.005	0	-.066	-.065	-.072	-.071	-.073
	4	124.4767	.005	.005	.006	.009	.009	.013	.013	.012	.013	.014	.012	.013	.013
	5	125.5068	.002	.002	.004	.006	.009	.013	.016	.022	.035	.044	.045	.050	.052
M22	2	127.5783	.004	.005	.008	.010	.012	.015	.019	.020	.026	--	--	--	--
	3	127.0714	.005	.006	.009	.015	.021	.031	.033	.038	.048	--	--	--	--
	4	127.2394	0	.005	.008	.011	.015	.019	.021	.023	.029	--	--	--	--
B1	2	126.1891	0	.002	.005	.011	.016	.019	.021	.021	.026	.029	.026	.029	--
	5	125.6496	.002	.001	.005	.007	.010	.014	.016	.017	.020	.023	.021	.023	--
B2	2	127.4831	.004	.005	.009	.012	.018	.023	.024	.026	.031	.035	.036	--	--
	3	126.5816	.005	.006	.012	.020	.027	.037	.040	.043	.054	.064	.067	--	--
B3	3	126.5924	-.009	-.011	-.007	-.006	-.003	0	.001	0	.004	.009	.007	--	--
	5	126.5092	-.004	-.006	-.004	0	.003	.008	.010	.012	.018	.027	.027	.038	--
CB1	4	124.9827	0	.002	.005	.006	.009	.013	.015	.016	.018	.018	.014	--	--
	5	124.9799	.001	.001	.004	.005	.008	.011	.012	.012	.016	.014	.012	.012	--
CB2	4	125.0616	.001	.001	.004	.007	.012	.018	.020	.024	.034	.041	.043	--	--
	5	124.8819	.002	.002	.006	.010	.014	.019	.022	.030	.044	.058	.061	--	--
CB3	1	126.1818	.004	.003	.006	.010	.017	.024	.025	.027	.029	.031	.029	.032	--
	2	125.9071	.003	.002	.006	.009	.012	.016	.016	.013	-.014	-.042	-.049	-.049	-.053
W1	3	123.8208	.003	.004	.007	.008	.012	.015	.010	.010	.013	.005	-.005	-.003	-.017
	4	123.6215	.001	.001	.003	.044	.007	.007	.007	.005	.005	.004	0	.005	--
W2	2	124.9798	-.005	-.007	-.004	-.002	.002	.006	.009	.012	.023	.027	.026	--	--
	3	125.0480	-.002	-.004	-.002	-.004	-.002	-.001	0	-.001	.001	-.001	-.005	--	--
W3	1	133.1486	.004	.003	.007	.011	.015	.018	.019	.021	.019	.018	.017	.018	--
	5	133.0197	.001	.001	.003	.004	.006	.007	.008	.007	.005	.005	.005	.015	--

TABLE 5. Cont.

Material	Sample Identi-fication	Starting Weight, g	Weight Change at Given Cycles, %												
			25	50	100	200	300	500	700	1000	1500	2000	2500	3000	3500
T1	3	120.9790	.004	.005	.008	.011	.014	.017	.019	.019	.023	.021	.006	--	--
	5	120.6744	.002	.003	.005	.008	.010	.011	.013	.012	.013	.009	-.008	--	--
T2	1	122.2966	.003	.005	.008	.011	.014	.018	.018	.020	.028	.024	.018	--	--
	3	122.6266	.002	.002	.004	.006	.009	.010	.011	.011	.014	.013	.007	--	--
T3	1	124.0487	.002	.002	.004	.007	.011	.012	.014	.016	.021	.024	.023	--	--
	3	124.1609	.002	.003	.006	.010	.014	.017	.019	.020	.027	.026	.024	--	--
M1	3	123.8115	.003	.004	.007	.010	.013	.015	.018	.018	.021	.021	.022	--	--
	4	124.6838	.002	.002	.005	.008	.012	.015	.018	.018	.023	.024	.027	--	--
M2	2	128.7011	.003	.004	.007	.011	.013	.016	.017	.018	.017	.016	.013	--	--
	5	128.5299	.002	.003	.008	.012	.015	.018	.018	.017	.009	.011	.008	.010	0
C1	1	125.5927	.003	.004	.005	.008	.010	.012	.013	.013	.010	.012	.016	.032	.033
	4	125.7833	.003	.004	.004	.006	.008	.009	.010	.011	.011	.005	.018	.043	.038

TABLE 6. ACCUMULATED THERMAL CYCLES TO FIRST CRACK INITIATION FOR TAZ-8A AND M22 ALLOYS AND VARIATIONS

Alloy	Specimen Identification	Cycles to First Crack: Small Radius, 0.64 mm (0.025 in.)	Cycles to First Crack: Large Radius, 1.02 mm (0.040 in.)
TAZ-8A	2	2750	--
TAZ-8A	4	2750	--
TAZ-8A	5	2250	--
M22	2	850	1250
M22	3	850	850
M22	4	850	850
B1	2	2250	--
B1	5	2250	--
B2	2	850	2250
B2	3	850	--
B3	3	1750	--
B3	5	850	2750
CB1	4	1750	--
CB1	5	2250	--
CB2	4	2250	--
CB2	5	1750	--
CB3	1	2750	--
CB3	2	3250	--
W1	3	2250	2250
W1	4	850	2250
W2	2	850	--
W2	3	1750	--
W3	1	2750	--
W3	5	2750	--
T1	3	850	--
T1	5	850	--
T2	1	2250	--
T2	3	1750	--
T3	1	1750	1750
T3	3	1750	1750
M1	3	1750	--
M1	4	1750	--
M2	2	2250	--
M2	5	3250	--
C1	1	>3500	>3500
C1	4	>3500	>3500

TABLE 7. SUMMARY OF CRACK PROPAGATION FOR TAZ-8A AND M22 ALLOYS AND VARIATIONS

Edge Radius, mm	Cycles	Crack Length, mm 1st Crack Front	1st Crack Back	1st Crack Average	2nd Crack Front	2nd Crack Back	2nd Crack Average	3rd Crack Front	3rd Crack Back	3rd Crack Average	Total Cracks Observed
					Specimen TA8-2						
Distance from bottom, mm				54.0			63.5			34.9	
0.71	2500	No cracks									0
	3000	--	.76	.38	.51	.25	.38				2
	3500	4.3	4.6	4.5	.76	.76	.76	2.3	4.8	3.6	4
					Specimen TA8-4						
Distance from bottom, mm				61.9							
0.71	2500	No cracks									0
	3000	5.3	5.6	5.5							1
	3500	6.1	7.4	6.8							1
					Specimen TA8-5						
Distance from bottom, mm				49.2			36.5			41.3	
0.69	2000	No cracks									0
	2500	.25	--	.13							1
	3000	3.6	3.6	3.6	.76	.76	.76	--	.51	.26	4
	3500	6.6	6.9	6.8	4.3	3.6	4.0	.51	.51	.51	4
					Specimen M22-2						
Distance from bottom, mm				36.5			66.7			71.4	
0.66	700	No cracks									0
	1000	1.5	.76	1.1	1.0	1.0	1.0	3.6	4.8	4.2	6
	1500	4.6	1.0	2.8	1.0	1.0	1.0	6.4	7.1	6.8	6
Distance from bottom, mm				31.8							
1.04	1000	No cracks									0
	1500	--	.25	.13							
Specimen removed after 1500 cycles.											

TABLE 7. Cont.

Edge Radius, mm	Cycles	Crack Length, mm: 1st Crack Front	1st Crack Back	1st Crack Average	2nd Crack Front	2nd Crack Back	2nd Crack Average	3rd Crack Front	3rd Crack Back	3rd Crack Average	Total Cracks Observed
				Specimen M22-3							
Distance from bottom, mm				41.3			27.0			68.2	
0.66	700	No cracks									0
	1000	4.1	5.3	4.7							1
	1500	6.9	8.1	7.5	.51	.51	.51	6.4	6.6	6.5	3
Distance from bottom, mm				33.3			61.9			25.4	
1.07	700	No cracks									0
	1000	.51	.51	.51	.25	--	.13				2
	1500	1.0	.51	.76	1.8	2.3	2.1	--	.51	.26	6
				Specimen M22-4							
Distance from bottom, mm				39.7			57.2			71.4	
0.66	700	No cracks									0
	1000	5.8	6.4	6.1	.25	.25	.25	.25	.25	.25	4
	1500	5.8	7.4	6.6	4.6	5.1	4.9	2.5	4.3	3.4	6
Distance from bottom, mm				31.8			49.2			39.7	
1.02	700	No cracks									0
	1000	1.0	.25	.63	1.0	1.5	1.3				2
	1500	1.0	1.0	1.0	3.8	3.6	3.7	.76	.76	.76	4
				Specimen M1-3							
Distance from bottom, mm				33.3			55.5			74.6	
0.61	1500	No cracks									0
	2000	.25	.25	.25	.51	.51	.51	.51	1.0	.76	6
	2500	4.6	4.6	4.6	5.8	5.6	5.7	7.1	6.4	6.8	7

Specimen removed after 2500 cycles.

TABLE 7. Cont.

Edge Radius, mm	Cycles	Crack Length, mm: 1st Crack Front	1st Crack Back	1st Crack Average	2nd Crack Front	2nd Crack Back	2nd Crack Average	3rd Crack Front	3rd Crack Back	3rd Crack Average	Total Cracks Observed
				Specimen M1-4							
Distance from bottom, mm				42.8			71.4			36.5	
0.69	1500	No cracks									0
	2000	.25	--	.13	6.9	7.6	7.3				2
	2500	1.5	1.8	1.7	8.9	8.4	8.7	4.8	4.8	4.8	4
Specimen removed after 2500 cycles.											
				Specimen M2-2							
Distance from bottom, mm				41.3							
0.71	2000	No cracks									0
	2500	7.9	8.1	8.0							1
Specimen removed after 2500 cycles.											
				Specimen M2-5							
Distance from bottom, mm				49.2							
0.71	3000	No cracks									0
	3500	.51	1.0	.76							1
				Specimen W1-3							
Distance from bottom, mm				33.3			68.2			46.0	
0.69	2000	No cracks									0
	2500	1.0	--	.50	3.3	2.8	3.1				2
	3000	1.0	--	.50	5.6	5.8	5.7	4.3	4.3	4.3	4
	3500	4.3	4.1	4.2	6.6	6.6	6.6	7.1	6.6	6.9	5
Distance from bottom, mm				46.0							
1.07	2500	No cracks									0
	3000	.51	.25	.33							1
	3500	.76	.25	.50							1
				Specimen W1-4							
Distance from bottom, mm				36.5			76.2			57.2	
0.71	700	No cracks									0
	1000	--	.51	.26	--	.25	.13				2
	1500	--	.51	.26	1.3	.76	1.0	1.3	.76	1.0	6
	2000	3.8	3.8	3.8	1.8	3.6	2.7	1.8	1.0	1.4	6
	2500	5.8	6.4	6.1	5.3	5.6	5.5	4.1	4.3	4.2	9
	3000	7.4	7.6	7.5	7.1	6.9	7.0	5.8	6.4	6.1	9

TABLE 7. Cont.

Edge Radius, mm	Cycles	Crack Length, mm 1st Crack Front	1st Crack Back	1st Crack Average	2nd Crack Front	2nd Crack Back	2nd Crack Average	3rd Crack Front	3rd Crack Back	3rd Crack Average	Total Cracks Observed
					Specimen W1-4						
Distance from bottom, mm				33.3			55.5			3.0	
1.09	2000	No cracks									0
	2500	1.3	2.5	1.9							1
	3000	4.1	4.3	4.2	2.5	--	1.3	2.8	3.1	3.0	6
Specimen removed after 3000 cycles.											
					Specimen W2-2						
Distance from bottom, mm				31.8			38.1			60.3	
0.66	700	No cracks									0
	1000	.76	.25	.51							1
	1500	3.8	4.1	4.0	.76	.25	.51				2
	2000	6.9	6.6	6.8	1.0	.76	.88				2
	2500	6.9	7.1	7.0	1.3	.76	1.0	5.3	5.8	5.6	3
Specimen removed after 2500 cycles.											
					Specimen W2-3						
Distance from bottom, mm				61.9			77.8			46.0	
0.66	1500	No cracks									0
	2000	4.6	4.6	4.6	4.8	5.3	5.1				2
	2500	6.1	6.1	6.1	6.6	7.1	6.9	2.8	3.6	3.2	4
Specimen removed after 2500 cycles.											
					Specimen W3-1						
Distance from bottom, mm				54.0			63.5				
0.69	2500	No cracks									0
	3000	5.1	5.1	5.1	6.9	7.4	7.2				2
Specimen removed after 3000 cycles.											
					Specimen W3-5						
Distance from bottom, mm				27.0			52.3				
0.76	2500	No cracks									0
	3000	1.8	1.5	1.7	8.9	8.6	8.8				2
Specimen removed after 3000 cycles.											

TABLE 7. Cont.

Edge Radius, mm	Cycles	Crack Length, mm — 1st Crack Front	1st Crack Back	1st Crack Average	2nd Crack Front	2nd Crack Back	2nd Crack Average	3rd Crack Front	3rd Crack Back	3rd Crack Average	Total Cracks Observed
				Specimen CB1-4							
Distance from bottom, mm				38.1			23.8				
0.64	1500	No cracks									0
	2000	2.3	2.5	2.4							1
	2500	6.9	7.4	7.2	.76	--	.38				2
Specimen removed after 2500 cycles.											
				Specimen CB1-5							
Distance from bottom, mm				31.8			61.9			76.2	
0.66	2000	No cracks									0
	2500	5.8	5.8	5.8	5.6	5.3	5.5				2
	3000	8.4	8.1	8.3	7.6	7.1	7.4	5.3	4.6	5.0	5
Specimen removed after 3000 cycles.											
				Specimen CB2-4							
Distance from bottom, mm				58.7							
0.69	2000	No cracks									0
	2500	7.1	7.1	7.1							1
Specimen removed after 2500 cycles.											
				Specimen CB2-5							
Distance from bottom, mm				30.1			46.0				
0.69	1500	No cracks									0
	2000	.25	.25	.25							1
	2500	.51	.51	.51	6.6	7.1	6.9				2
Specimen removed after 2500 cycles.											
				Specimen CB3-1							
Distance from bottom, mm				30.1			61.9			69.9	
0.66	2500	No cracks									0
	3000	3.6	4.6	4.1	.51	--	.26	.51	1.0	.76	3
				Specimen CB3-2							
Distance from bottom, mm				39.7			44.5			63.5	
0.64	3000	No cracks									0
	3500	4.6	5.1	4.9	.51	--	.26	.51	1.0	.76	3

TABLE 7. Cont.

Edge Radius, mm	Cycles	Crack Length, mm 1st Crack Front	1st Crack Back	1st Crack Average	2nd Crack Front	2nd Crack Back	2nd Crack Average	3rd Crack Front	3rd Crack Back	3rd Crack Average	Total Cracks Observed
					Specimen T1-3						
Distance from bottom, mm				28.6			69.9			55.5	
0.69	700	No cracks									0
	1000	.25	--	.12	1.3	.51	.92				2
	1500	.51	--	.26	6.4	6.9	6.7	2.5	2.5	2.5	5
	2000	5.1	5.3	5.2	8.1	8.4	8.3	4.6	4.6	4.6	7
	2500	6.4	7.6	7.0	9.1	9.4	9.3	5.6	5.3	5.5	7
Specimen removed after 2500 cycles.											
					Specimen T1-5						
Distance from bottom, mm				31.8			52.3			68.2	
0.66	700	No cracks									0
	1000	.25	.51	.38	--	.51	.26				2
	1500	3.1	4.6	3.9	4.3	4.1	4.2				2
	2000	8.4	7.9	8.2	6.9	6.6	6.8	1.3	1.5	1.4	4
	2500	8.4	8.6	8.5	7.6	7.1	7.4	8.6	8.6	8.6	4
Specimen removed after 2500 cycles.											
					Specimen T2-1						
Distance from bottom, mm				30.1			42.8				
0.66	2000	No cracks									0
	2500	3.1	3.3	3.2	7.6	6.4	7.0				2
Specimen removed after 2500 cycles.											
					Specimen T2-3						
Distance from bottom, mm				30.1			47.6			71.4	
0.69	1500	No cracks									0
	2000	.76	1.3	1.0	7.9	6.6	7.3	5.3	6.4	5.9	3
	2500	6.1	5.6	5.9	7.9	7.9	7.9	7.9	8.6	8.3	3
Specimen removed after 2500 cycles.											
					Specimen T3-1						
Distance from bottom, mm				33.3			50.8			66.7	
0.69	1500	No cracks									0
	2000	2.5	2.3	2.4	1.0	1.5	1.3	.51	.25	.38	8
	2500	5.6	5.3	5.5	6.4	5.8	6.1	5.3	5.3	5.3	8

TABLE 7. Cont.

Edge Radius, mm	Cycles	Crack Length, mm — 1st Crack: Front	1st Crack: Back	1st Crack: Average	2nd Crack: Front	2nd Crack: Back	2nd Crack: Average	3rd Crack: Front	3rd Crack: Back	3rd Crack: Average	Total Cracks Observed
				Specimen T3-1							
Distance from bottom, mm				58.7							
1.07	1500	No cracks									0
	2000	.25	.25	.25							1
	2500	.51	.25	.38							1
Specimen removed after 2500 cycles.											
				Specimen T3-3							
Distance from bottom, mm				31.8			41.3			54.0	
0.69	1500	No cracks									0
	2000	3.6	3.6	3.6	.51	.76	.64	.51	.25	.38	5
	2500	6.6	6.4	6.5	2.0	1.3	1.7	7.1	7.4	7.3	6
Distance from bottom, mm				34.9			66.7				
1.02	1500	No cracks									0
	2000	.76	--	.38							1
	2500	.76	.25	.51	--	.25	.13				2
Specimen removed after 2500 cycles.											
				Specimen B1-2							
Distance from bottom, mm				31.8			49.2			60.3	
0.56/0.61	2000	No cracks									0
	2500	1.0	1.0	1.0	3.8	4.6	4.2	.25	1.0	.63	3
	3000	6.6	7.1	6.9	7.1	7.1	7.1	3.1	3.8	3.5	7
Specimen removed after 3000 cycles.											
				Specimen B1-5							
Distance from bottom, mm				49.2			31.8			60.3	
0.61/0.71	2000	No cracks									0
	2500	2.5	2.5	2.5							1
	3000	7.1	7.1	7.1	6.6	7.1	6.9	3.1	3.8	3.5	7
Specimen removed after 3000 cycles.											

TABLE 7. Cont.

Edge Radius, mm	Cycles	Crack Length, mm: 1st Crack Front	1st Crack Back	1st Crack Average	2nd Crack Front	2nd Crack Back	2nd Crack Average	3rd Crack Front	3rd Crack Back	3rd Crack Average	Total Cracks Observed
					Specimen B2-2						
Distance from bottom, mm				27.0			52.3			71.4	
0.66	700	No cracks									0
	1000	.25	--	.13	.51	--	.26	.25	--	.13	4
	1500	.51	--	.26	1.5	.25	.88	.25	--	.13	6
	2000	1.3	.25	.78	5.1	5.6	5.4	1.0	.51	.76	9
	2500	7.6	7.6	7.6	7.9	8.1	8.0	3.6	3.6	3.6	12
Distance from bottom, mm				49.2			69.9				
0.99	2000	No cracks									0
	2500	--	.76	.39	.25	1.8	1.0				2
Specimen removed after 2500 cycles.											
					Specimen B2-3						
Distance from bottom, mm				31.8			36.5			42.8	
0.60	700	No cracks									0
	1000	.51	.25	.38	.25	--	.13	.51	.25	.38	5
	1500	1.8	.25	1.0	3.6	3.1	3.4	.51	.25	.38	8
	2000	1.8	.25	1.0	6.4	6.1	6.3	.51	.25	.38	9
	2500	1.8	.25	1.0	7.9	8.1	8.0	4.6	4.8	4.7	9
Specimen removed after 2500 cycles.											
					Specimen B3-3						
Distance from bottom, mm				34.9			65.1				
0.66	1500	No cracks									0
	2000	4.3	2.5	3.4	3.8	3.3	3.6				2
	2500	5.8	5.8	5.8	6.9	6.6	6.8				2
Specimen removed after 2500 cycles.											

TABLE 7. Cont.

Edge Radius, mm	Cycles	Crack Length, mm									Total Cracks Observed
		1st Crack			2nd Crack			3rd Crack			
		Front	Back	Average	Front	Back	Average	Front	Back	Average	
Specimen B3-5											
Distance from bottom, mm				30.1			42.8			61.9	
0.61	700	No cracks									0
	1000	--	.25	.13	--	.25	.13	--	.25	.13	4
	1500	.51	.51	.51	.25	.51	.38	--	.25	.13	8
	2000	.76	1.3	1.0	.51	.51	.51	.76	.51	.64	8
	2500	2.0	2.3	2.2	2.0	2.0	2.0	3.8	3.1	3.5	9
	3000	6.6	6.4	6.5	5.1	4.6	4.9	6.6	5.8	6.2	11
Distance from bottom, mm				39.7			57.2			66.7	
1.04	2500	No cracks									0
	3000	3.8	3.3	3.6	.51	.25	.38	1.0	1.5	1.3	3
Specimen removed after 3000 cycles.											

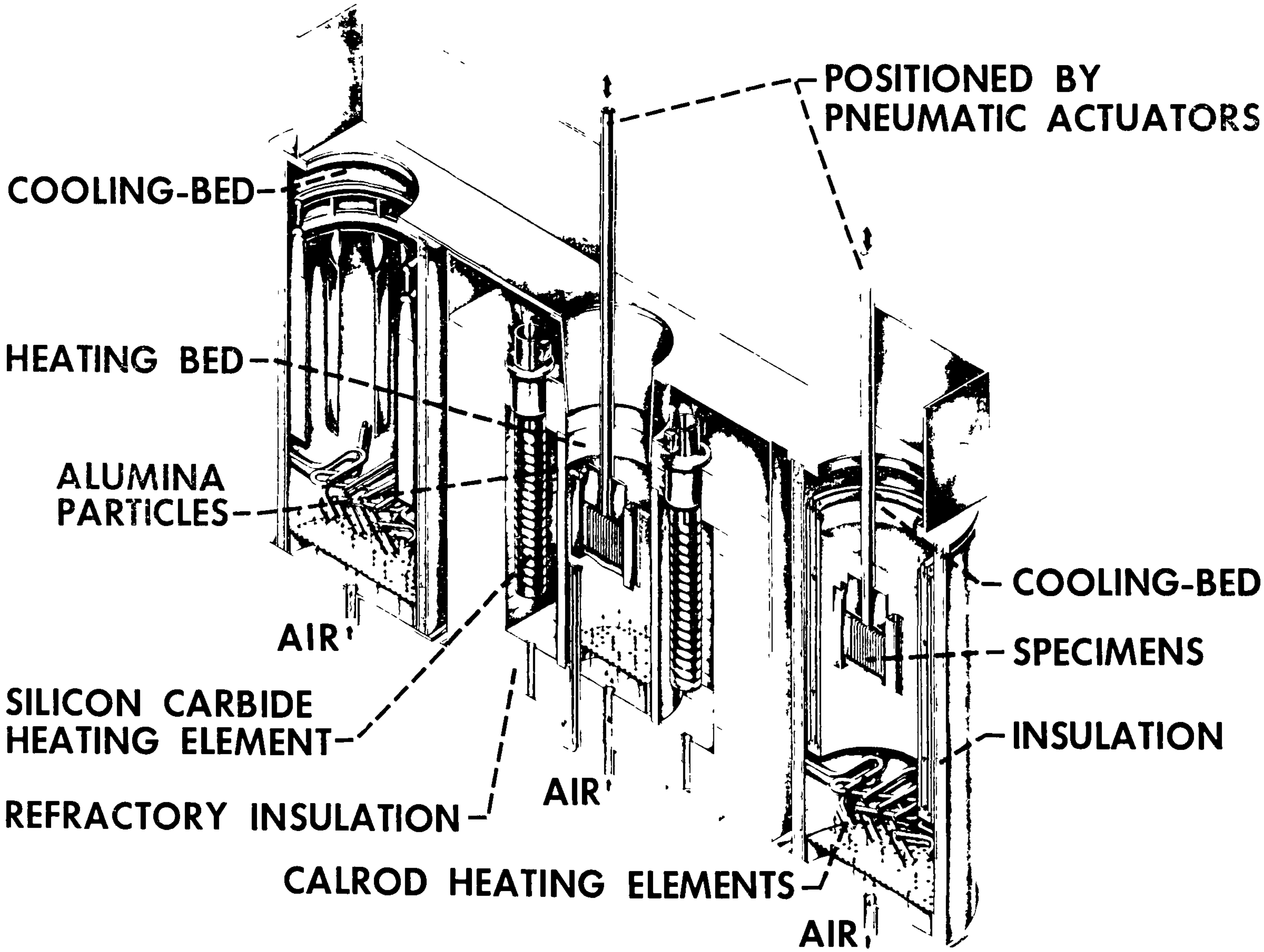

Figure 1. Fluidized bed thermal fatigue facility.

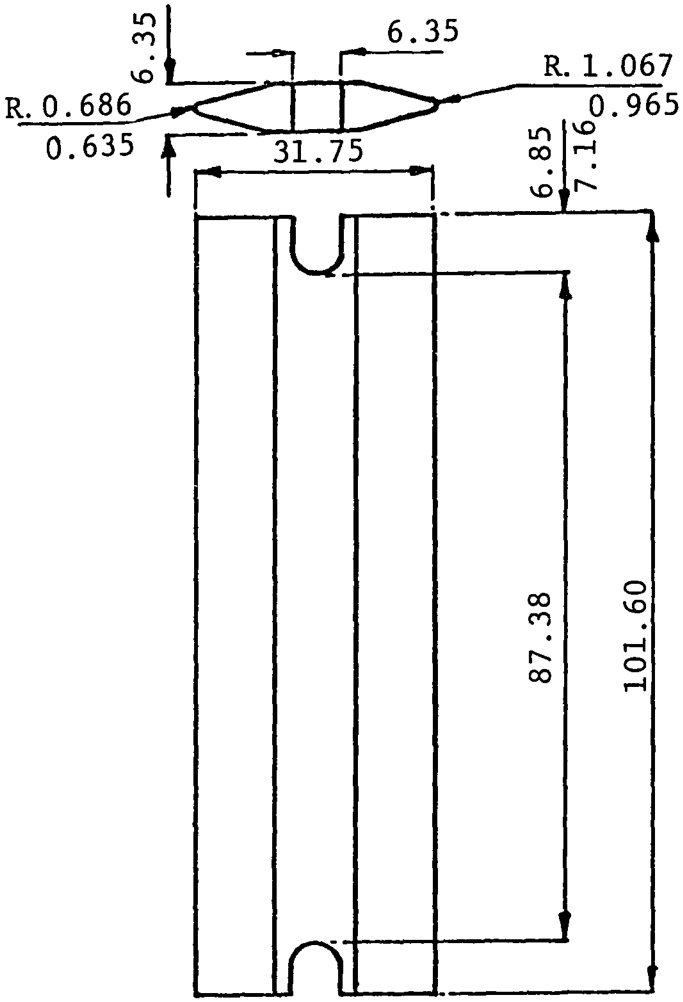

(a) Double-edge wedge specimen
(dimensions in mm)

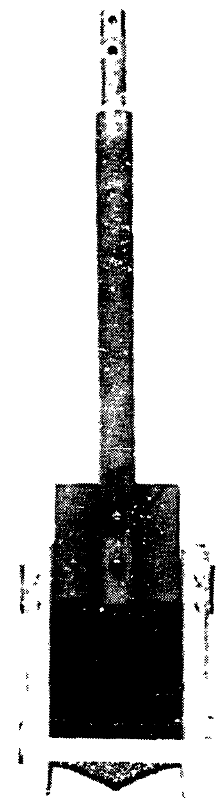

Neg. No. 45935 X 1/12

(b) Holding fixture

Figure 2. Double-edge wedge test specimen and holding fixture.

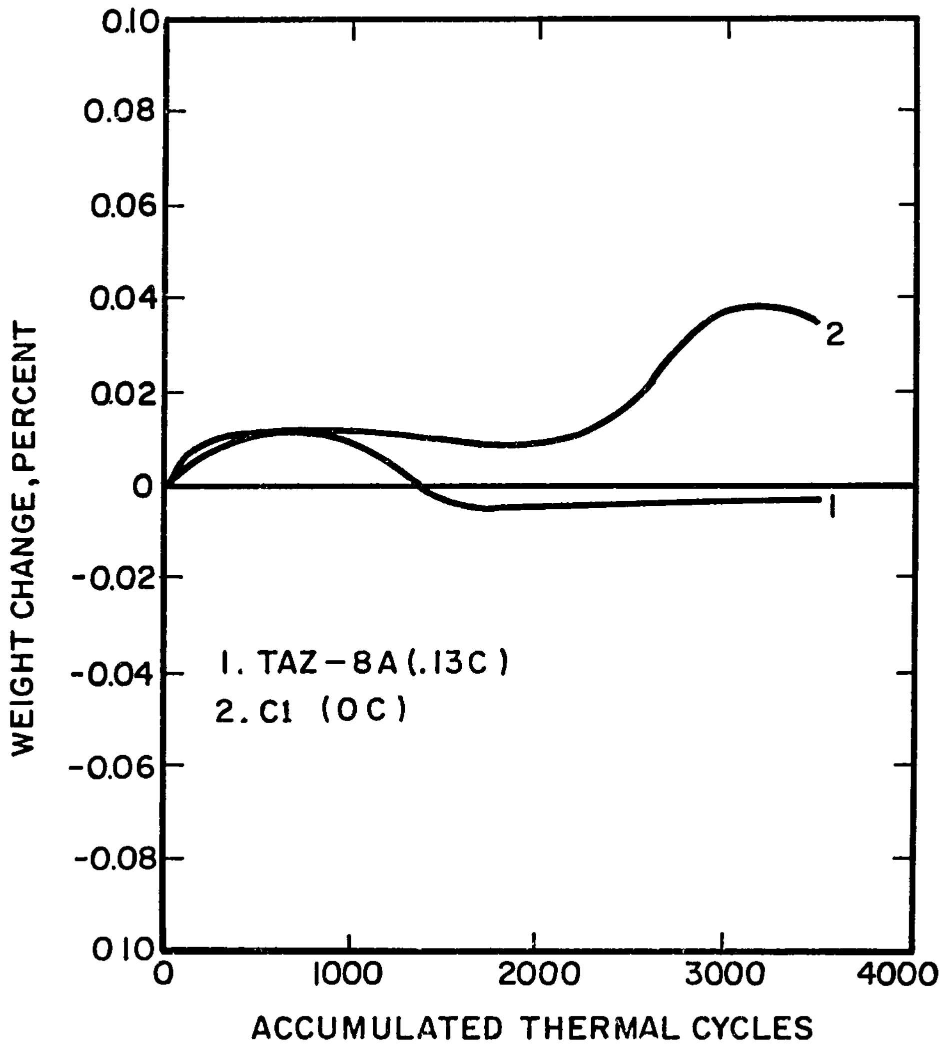

Figure 3. Percent weight change versus accumulated thermal cycles for alloy variations of TAZ-8A and M22, effect of variations of carbon content.

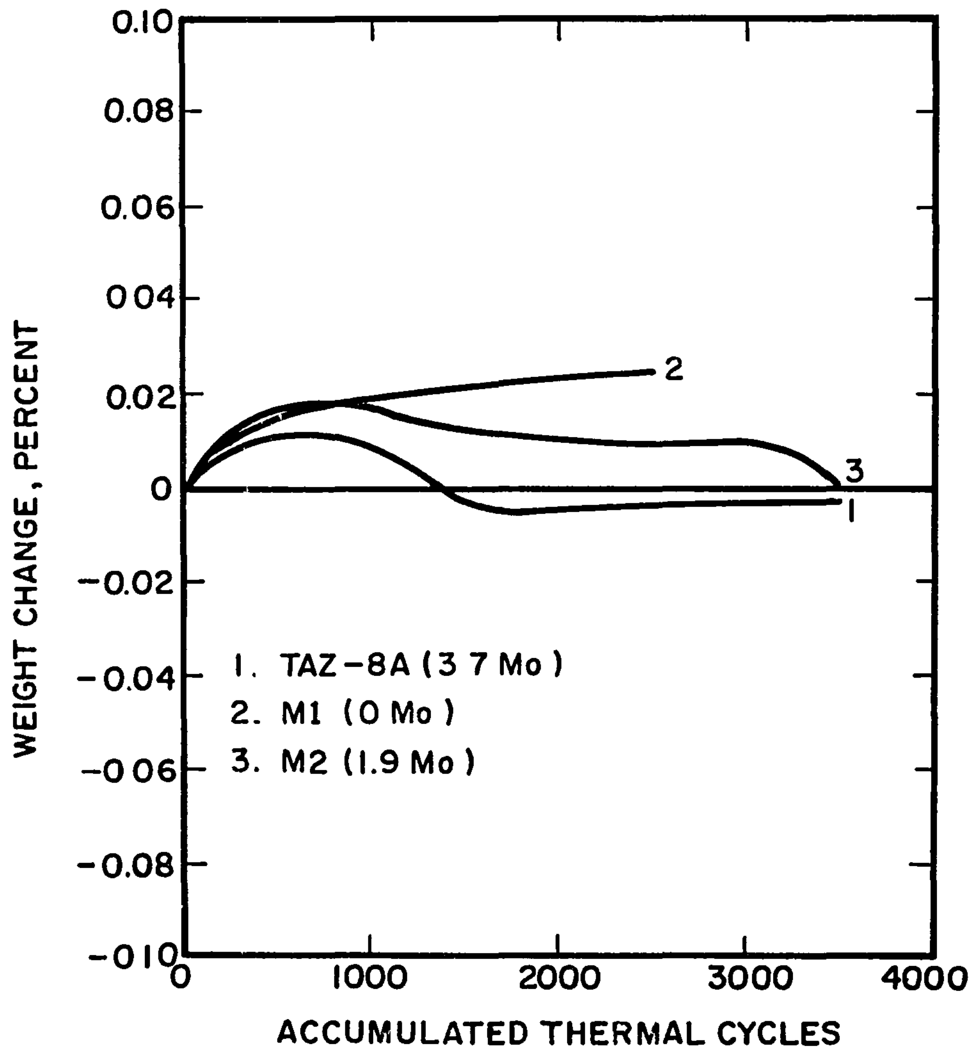

Figure 4. Percent weight change versus accumulated thermal cycles for alloy variations of TAZ-8A and M22, effect of variations of molybdenum content.

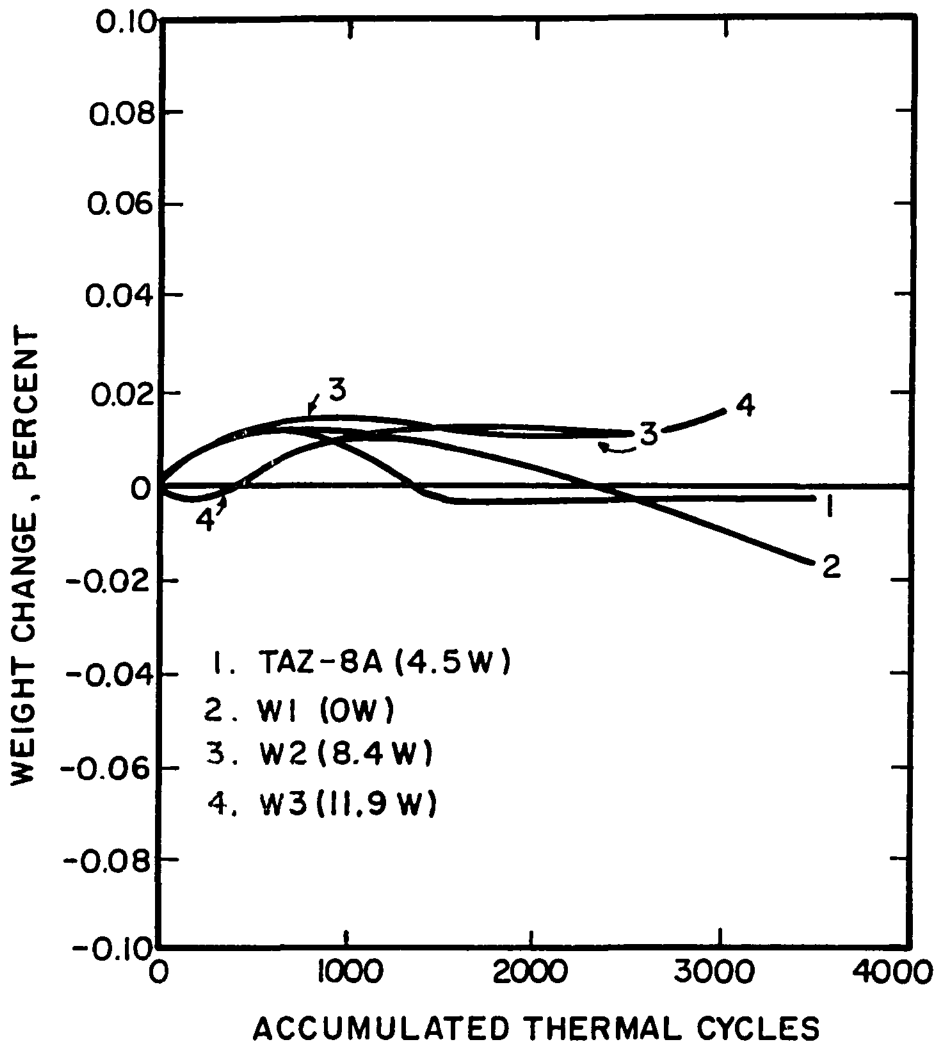

Figure 5. Percent weight change versus accumulated thermal cycles for alloy variations of TAZ-8A and M22, effect of variations of tungsten content.

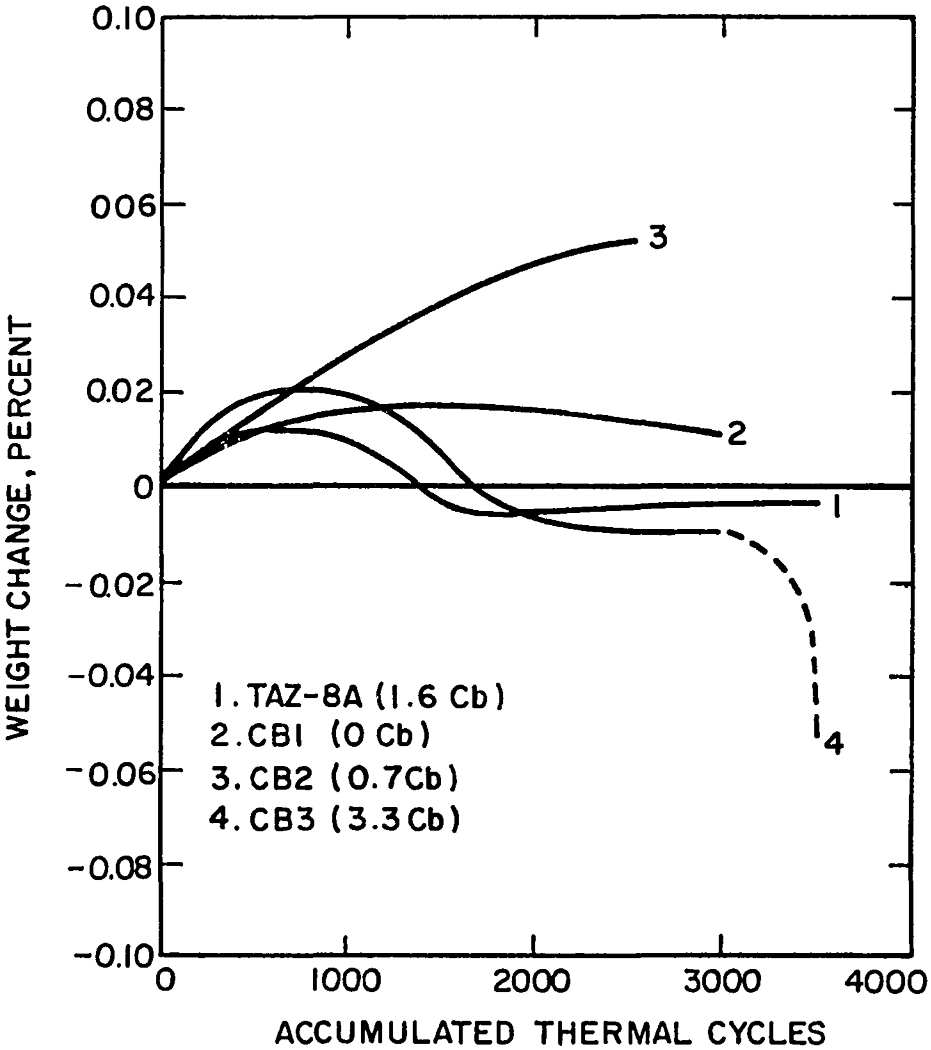

Figure 6. Percent weight change versus accumulated thermal cycles for alloy variations of TAZ-8A and M22, effect of variations of columbium content. (Dashed line indicates single value data.)

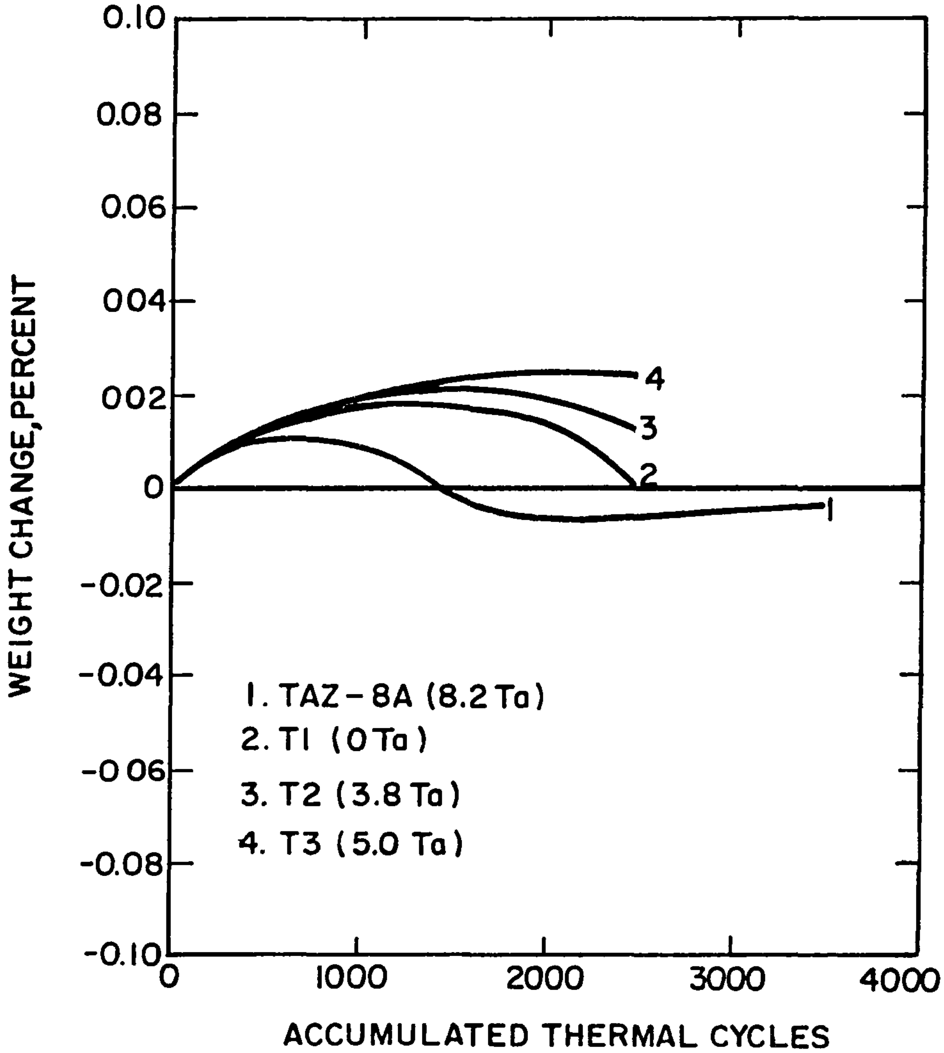

Figure 7. Percent weight change versus accumulated thermal cycles for alloy variations of TAZ-8A and M22, effect of variations of tantalum content.

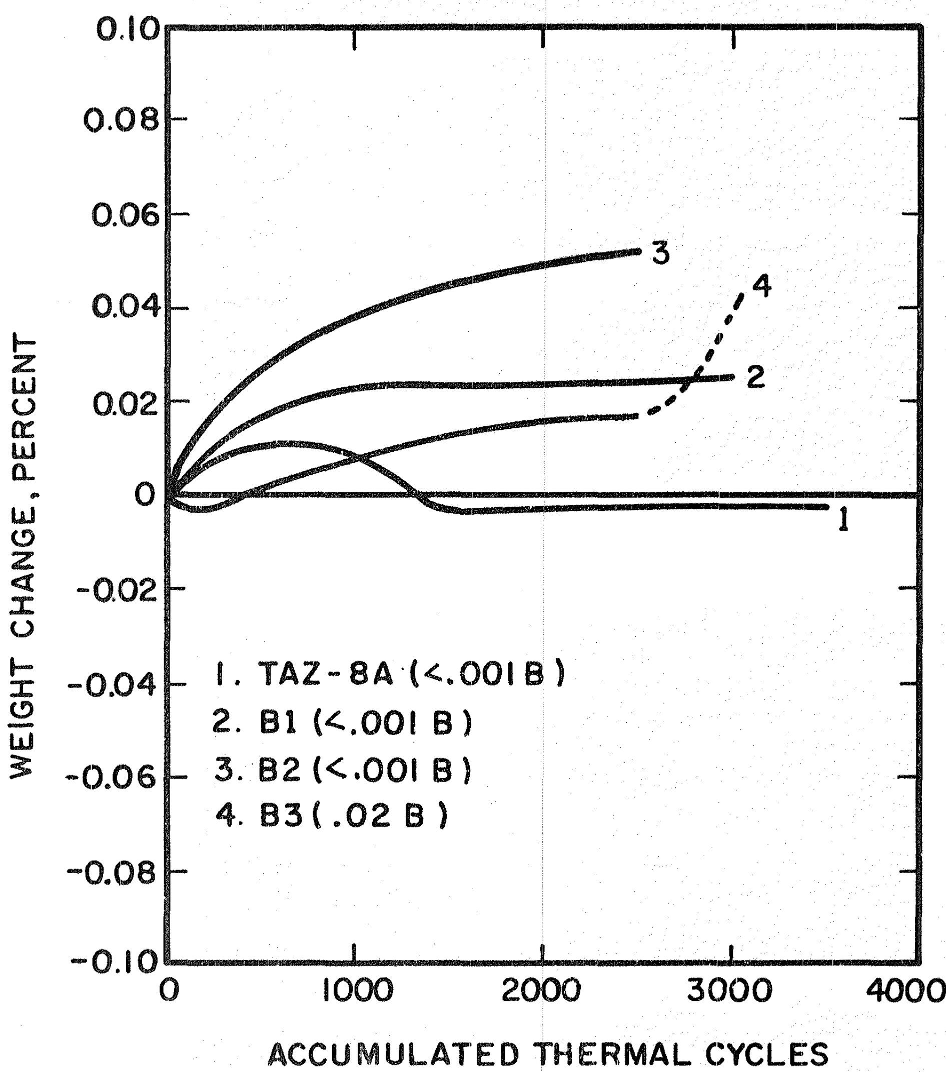

Figure 8. Percent weight change versus accumulated thermal cycles for alloy variations of TAZ-8A and M22, effect of variations of boron content. (Dashed line indicates single value data.)

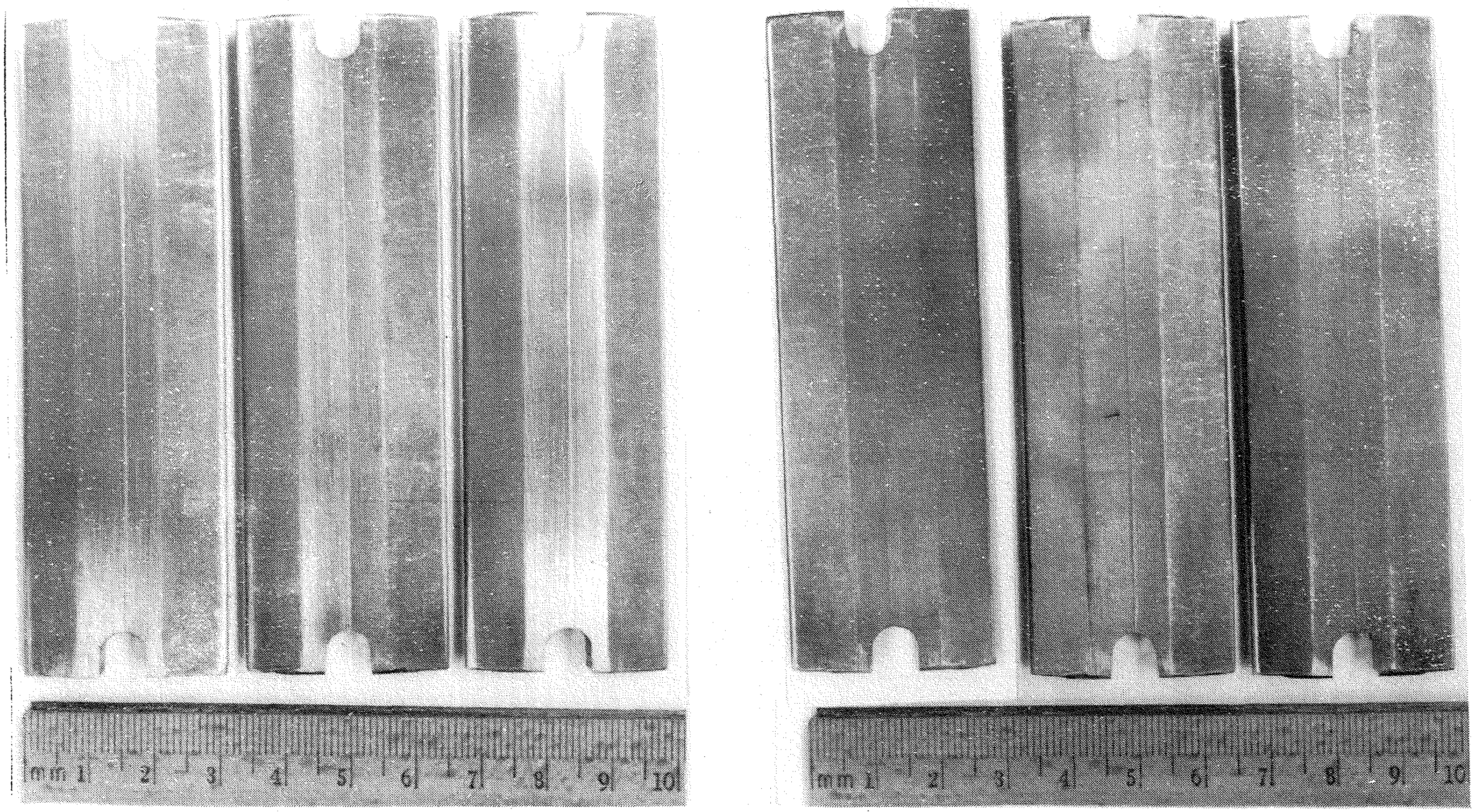

Neg. No. 51927 1X
2 4 5
(a) Alloy TAZ-8A

Neg. No. 51926 1X
2 3 4
(b) Alloy M22

Figure 9. Typical appearance of experimentally fabricated TAZ-8A and M22 alloys double-edge wedge specimens as-received. (The small radius is at the right.)

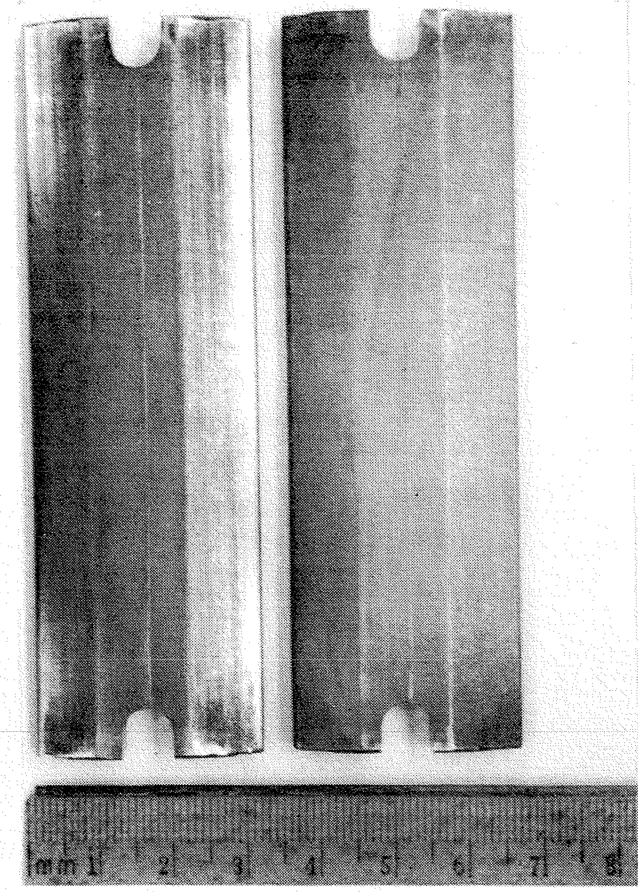

Neg. No. 51919 IX

3 4

(a) Alloy Variation W1

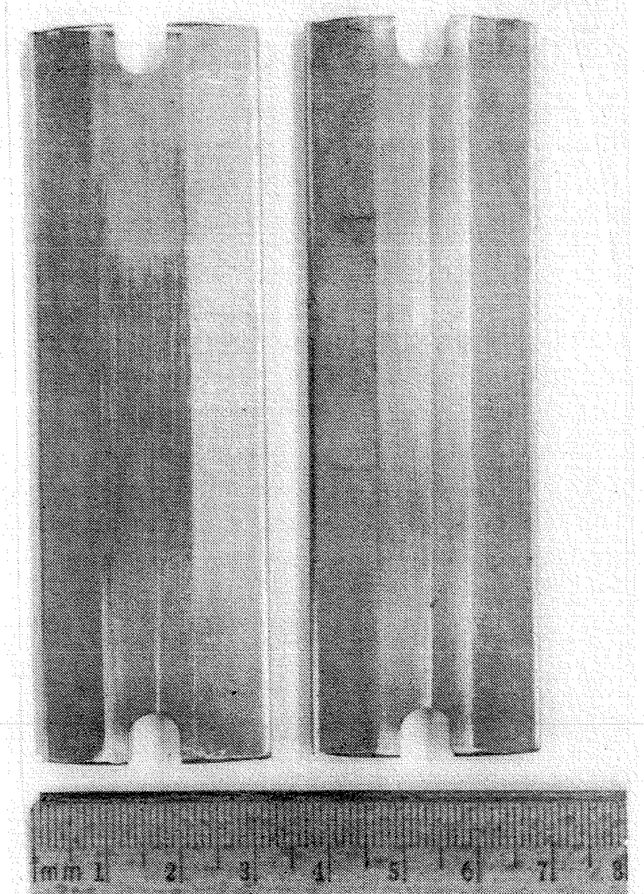

Neg. No. 51916 IX

3 5

(b) Alloy Variation T1

Figure 10. Typical appearance of W1 and T1 alloy variations double-edge wedge specimens as-received. (The small radius is at the right.)

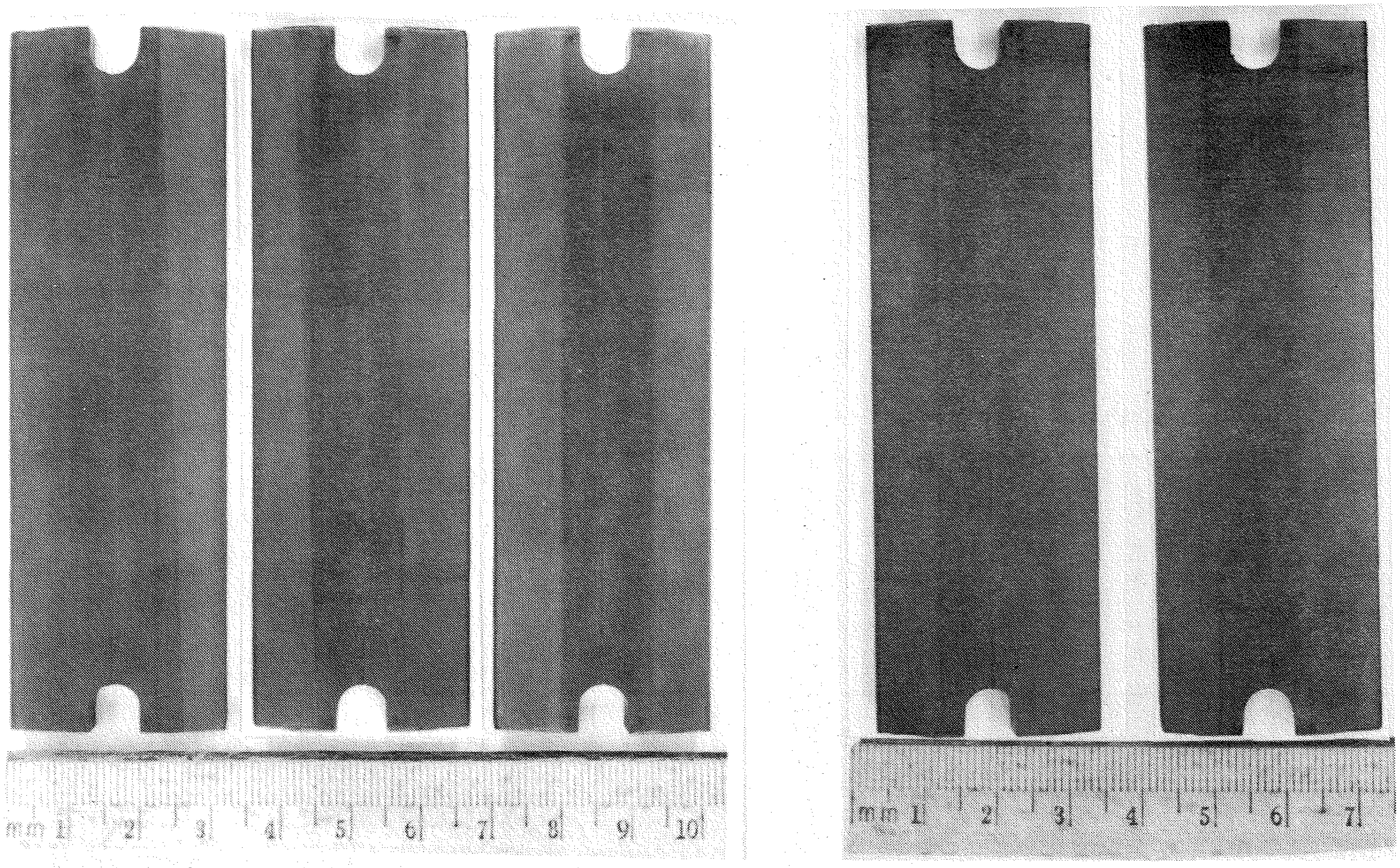

Neg. No. 52267 1X

2 3 4

(a) Alloy M22 (1500 Cycles)

Neg. No. 52264 1X

2 3

(b) Alloy Variation B2 (2500 Cycles)

Figure 11. Appearance of selected specimens after indicated thermal cycles. (The small radius is at the right.)

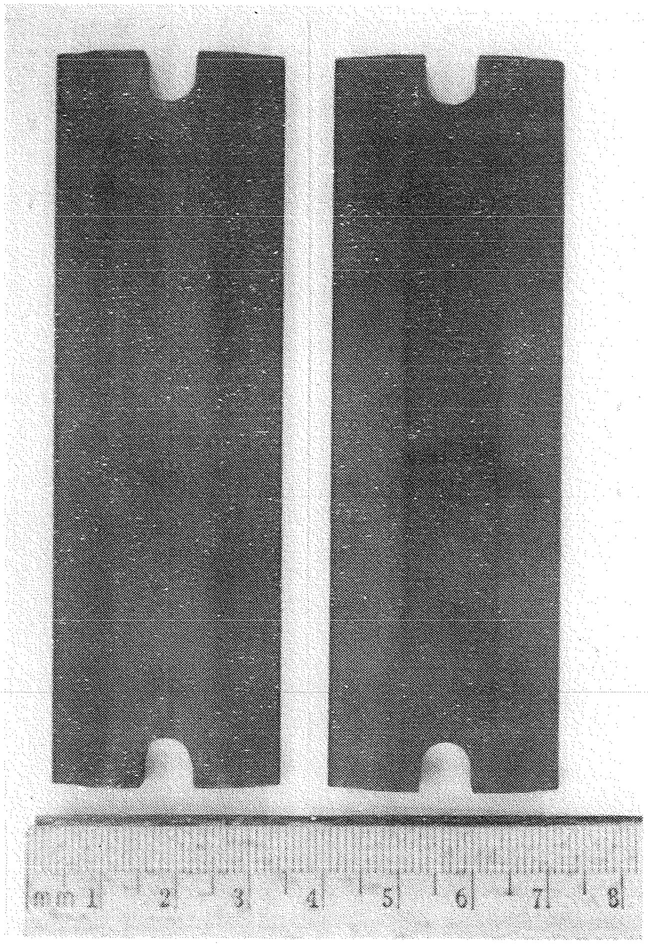

Neg. No. 52261 1X

3 (3500 Cycles) 4 (3000 Cycles)

(a) Alloy Variation W1

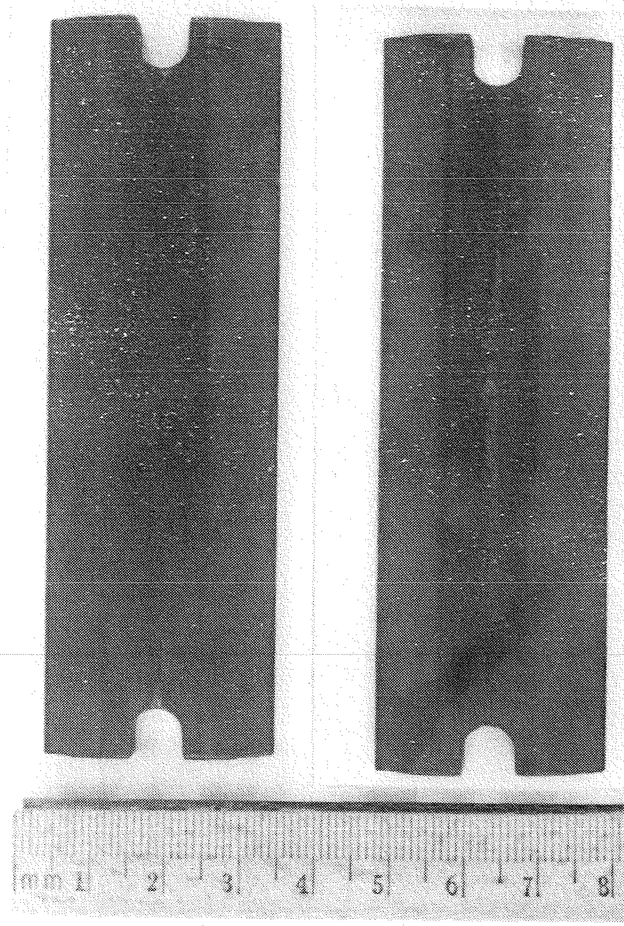

Neg. No. 52257 1X

3 5

(b) Alloy Variation T1 (2500 Cycles)

Figure 11. Cont.

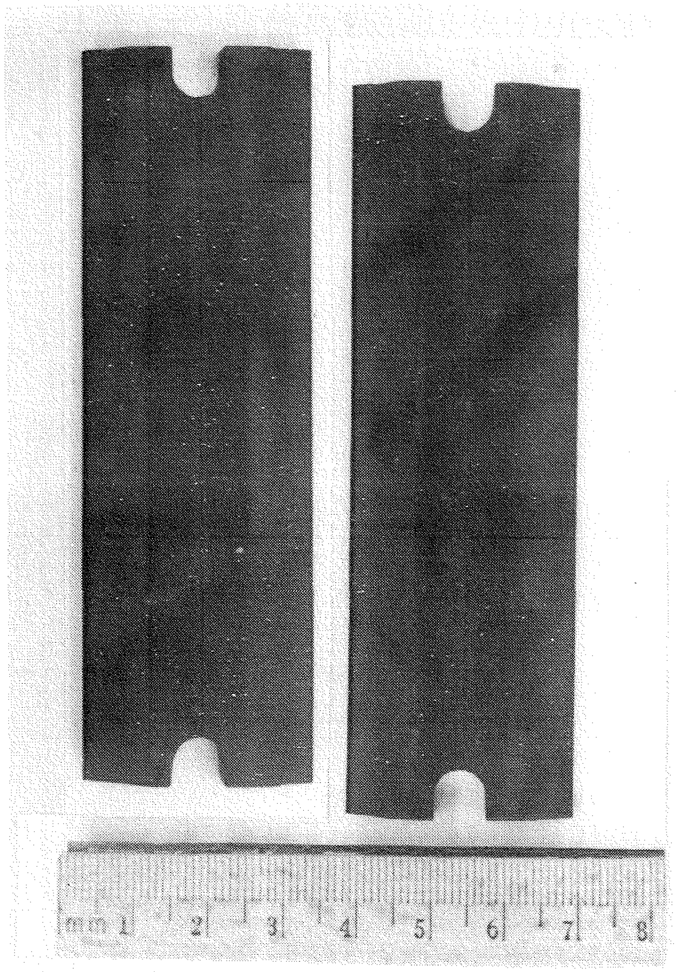

Neg. No. 52260 1X

4 (2500 Cycles) 5 (3000 Cycles)

(a) Alloy Variation CB1

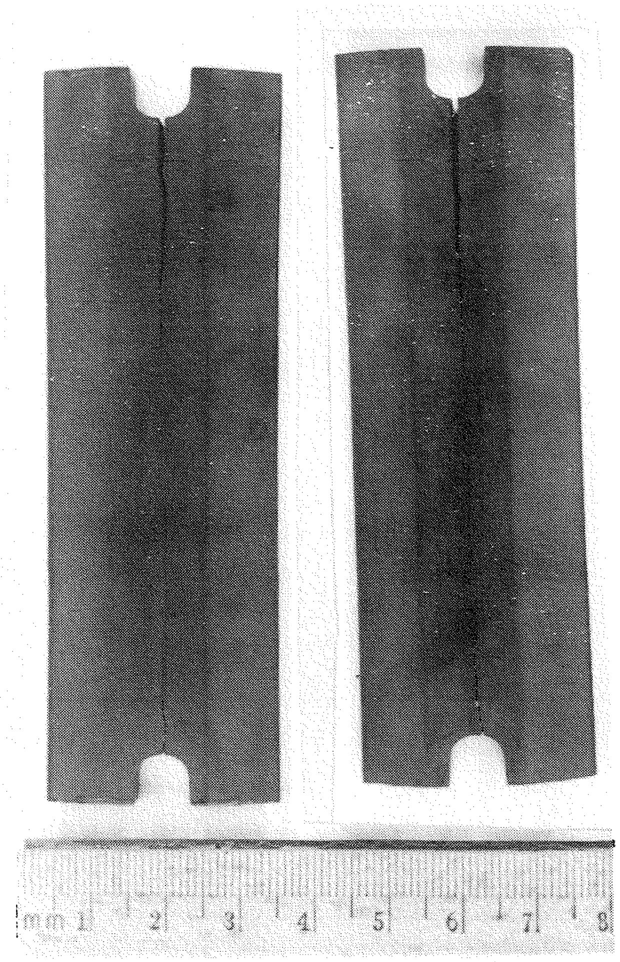

Neg. No. 52252 1X

1 4

(b) Alloy Variation C1 (3500 Cycles)

Figure 11. Cont.

End of Document